

N 71-12962

**NASA TECHNICAL
MEMORANDUM**

NASA TM X-52939

NASA TM X-52939

**CASE FILE
COPY**

**PRESSURE MEASUREMENTS IN THE EXHAUST OF A PULSED
MEGAWATT MPD ARC THRUSTER**

by Charles J. Michels and Thomas M. York
Lewis Research Center
Cleveland, Ohio

TECHNICAL PAPER proposed for presentation at
Ninth Aerospace Sciences Meeting sponsored by the
American Institute of Aeronautics and Astronautics
New York, New York, January 25-27, 1971

PRESSURE MEASUREMENTS IN THE EXHAUST OF A PULSED MEGAWATT MPD ARC THRUSTER

Charles J. Michels
National Aeronautics and Space Administration
Lewis Research Center
Cleveland, Ohio

and Thomas M. York*
The Pennsylvania State University
University Park, Pennsylvania

Abstract

Transient exhaust pressure history shows a large initial pressure pulse (30 μ sec wide) followed by lower order signals. The variation of this pulse with source parameters and duct position is discussed. The peak dynamic pressures are of order 10^4 N/m² and static pressures are about 10^2 N/m². At a fixed position, the pulse increases with power, and/or magnetic field. Generally, the pulse occurs: about 10 microseconds after plasma light arrives, about 10 to 50 microseconds before plume current arrives and Faraday cup signals occur. This narrow neutral pulse dominates the time integrated pressure for approximately 100 microseconds.

Introduction

In the literature on MPD-ARC thrusters, distinctions are made between starting transients, quasi-steady conditions, and steady, D.C. like, operation. These distinctions are important because the dominant physics of the processes might well be different for each case. Most investigators have not examined the starting transients of MPD ARC thrusters. It has been assumed that quasi-steady operation (equivalent to steady operation for much of the pulse time) could be achieved in a time of the order of 10^{-5} seconds. This assumption seemed to be justified by experimental observations, plasma light, probe traces, or terminal characteristics that appeared to be quite steady, at least for the 100 microsecond time periods or so described in Refs. 1 to 4. Brief qualitative descriptions are made of the starting transients as depicted in plasma light traces,⁽⁴⁾ probe traces,⁽³⁾ and terminal characteristics.⁽¹⁻³⁾

Quasi-steady single pulse operation has been examined in more detail at high power level since thrusters having such pulses have possible application. Also, if "steady" operation could be attained for a single pulse then very high power operation can be simulated without the problems of anode cooling and large power supplies needed for steady-state operation. Studies at Princeton University,⁽⁵⁻⁹⁾ Langley Research Center,⁽¹⁰⁾ Lewis Research Center,^(4,11) University of California, San Diego,^(2,12) and at Avco Corporation⁽¹³⁾ all examined details of quasi-steady operation (100 to 200 μ sec duration).

In this paper results of transient pressure measurements in the exhaust are presented. The time-varying nature of exhaust pressure (for 100 μ sec) is discussed. The relation between starting transient pressure and later pressure for the 100 to 200 microsecond test times is described. The significance of these and other measurement for understanding the physical processes in high power MPD-ARC thrusters is evaluated.

*NASA Summer Faculty Fellow.

Apparatus

Capacitor Bank

The thruster was energized by a 10 kilojoule capacitor bank. Details of the capacitor bank are described in Ref. 4. After the bank switch was closed, arc current was allowed to develop to its peak value (21 μ sec). Then a crowbar switch was closed, forcing current to decay monotonically with time. The L/R decay time ranged from 250 to 350 microseconds depending on arc resistance. This allowed an almost linear decay of arc current for 100 microseconds after crowbar time. It is during this time that the data was gathered.

Plasma Thruster

A photograph of the single-shot thruster is shown in Fig. 1. The arc chamber is hidden from view at the center of the toroidal dewar for the superconducting magnet. The magnet is used to supply the auxiliary magnetic field for the accelerator. Plasma flows to the right from the thruster into a 15 centimeter inside diameter evacuated glassware system.

Prior to operating the thruster, the magnet dewar was filled with liquid helium, and after it became cold the magnet wire became superconducting. Then the magnet was energized to a given magnetic field setting (0 to 2.0 T) and maintained at that condition for the testing period. The capacitor bank was charged next. It was not switched until propellant had properly filled the arc chamber (650 μ sec). For operational convenience, the cathode was not preheated for the experiments described here.

Nitrogen propellant was introduced into the arc chamber by a high speed gas valve that was operated by an electromagnetic actuator. All tests were run at 7 g/sec nitrogen. The transient, cold flow, gas pressure in the arc chamber was measured by a commercially available piezoelectric pressure transducer in a previous experiment. That pressure and the orifice equations for steady flow were used to calculate the mass flow rate for all the tests of this report. From the transient pressure records it was found that stable flow occurred after 650 microseconds. The arc was started at that time. Thereafter, a transient plasma flows for a few hundred microseconds into the evacuated glassware section.

A cross-sectional view of the arc chamber is shown in Fig. 2. An iron filings map of the magnetic field is also shown. The cathode is a tungsten ribbon measuring 1 cm wide, 2 cm long, and 1 mm thick. The anode is a 4.2 cm inside diameter copper ring.

A sequence controller actuates gas puff injection, delay for gas distribution, bank switch closure, crowbar switch closure, and then data gathering "start" times. The system can be recycled every two minutes. A series of 500 separate shots were gathered for this report. Prior to data gathering, a similar number of shots were made to proof the instruments and select interesting data areas.

Instrumentation

Piezoelectric pressure probe. - The possibility of carrying out detailed diagnostics of pressure in transient plasma discharges has been considered by one of the authors⁽¹⁴⁾ and the optimum effectiveness of piezoelectric transducers was determined. The design and response of unique high performance transducers for this application has also been reported.⁽¹⁵⁾ This probe concept utilizes a piezoelectric ceramic element supported on a structure of backing rod in an insulated housing (fig. 3). Based on earlier investigations of the discharge environment⁽⁴⁾ two probing units were fabricated, both using PZT-5A (Clevite Corp.) piezo-ceramic: a low frequency, high sensitivity probe with sensing surface 1.25 cm in diameter, o.d. 1.9 cm, 60 μV per N/m^2 output, and 2.5 μsec risetime; a high frequency, low sensitivity unit with 0.64 cm sensing diameter, 1.25 cm o.d., 15 μV per N/m^2 output, and 0.4 μsec risetime. In each case the sensing surface was electrically insulated by a thin layer (~0.1 cm) of epoxy with a definable signal delay time of ~0.2 μsec . This figure combined with the specified risetime values is an order of magnitude smaller in time than the event being considered. The output of these units was calibrated in a simple shock tube fabricated for that purpose, with a 2.85 cm diameter i.d., 1.0 m long driver and driven sections. Low frequency response with $1.0 \times 10^5 \text{ N}/\text{m}^2$ (15.0 psia) air driven by 42.0 psia helium is presented in Fig. 4. Concerning the low frequency response, a calculated RC time constant of 650 μsec for the probe system was verified experimentally in the shock tube tests.

For the probing units installed in the MPD-ARC discharge apparatus, an emitter follower (fig. 5) was utilized to avoid excessive signal attenuation. In order to more precisely define trends in the pressure data, an electronic low-pass filter (Spectrum Analog Electronic Filter Type H-18) was used at times; corrections for signal delay and attenuation could be accounted for reasonably accurately in those cases when utilized. Figure 6 shows a comparison of typical filtered and unfiltered pressure traces. In order to distinguish real gas-kinetic pressure signals from spurious response, several steps were taken. A "dummy" probe structure without active sensing elements was used to evaluate electromagnetic pickup; this proved to be negligible on the scale of the data signal. Extraneous response due to accelerations in the thruster-probe system was evaluated with an active sensing probe, capped to deny contact with the plasma. Acceleration signals were measurable and of lower order; they were recorded for every data condition. These tare readings were then subtracted from records with plasma contact to obtain gas-kinetic pressure values. In order to control spurious stress oscillations in the probe body,⁽¹⁵⁾ a soft rubber collar of 3.2 cm

diameter was at times fitted over the low frequency probe body. Interference effects proved to be negligible, allowing a more precise determination of plasma pressure values.

Rogovsky loop. - A glass tubing enclosed Rogovsky loop, with 2.5 cm inside diameter sensing area, was used to measure gross currents flowing in the discharge that threads the loop. The loop was aligned so that its leading edge was positioned at the same axial station and usually at a duct radius position equal but opposite to the pressure probe location. Thus, simultaneous loop and pressure traces could be gathered. The loop signal was actively integrated and then presented on an oscilloscope. The active area of the loop was normal to the duct radius, it thus intercepted radial components of the plume currents. Calibration was accomplished by passing a wire carrying a transient current through both the loop and a PEARSON CURRENT TRANSFORMER used as a secondary standard for calibrations. Typical calibration traces are shown in Fig. 7. These calibration tests show that the signal amplitude and waveshape are well preserved for the time durations of these tests.

Faraday cup probe. - A Faraday cup probe was used to collect ions from the streaming plasma. It was biased with a 45 V battery so as to repel electrons. Various pin holes could be used. This probe was used in much the same manner as that discussed in Ref. 4, except that a better attempt was made to keep not only the electronics but the measuring oscilloscope floating. The amplifiers were also much faster. 1.0 microsecond response times were achieved to obtain better "arrival time" details of the ions streaming in the exhaust.

Results and Discussion

Cold Flow Total Pressure

The low frequency piezo-pressure probe was used to measure "cold" gas flow in the duct. The propellant was injected without starting the arc. At the data gathering times used in this report, the cold gas propellant total pressure is two orders of magnitude less than the measured pressures for the powered case. Specifically, at arc initiation time the total pressure magnitude on axis at a distance downstream from the anode face of 5 cm ($Z = 5 \text{ cm}$) is $340 \text{ N}/\text{m}^2$, while farther downstream, on axis, at $Z = 30 \text{ cm}$, the total pressure sensed is $6 \text{ N}/\text{m}^2$ (see fig. 8). Supplementary measurements indicate static pressures are approximately one-tenth of the total cold gas pressure. The pressure front noted in Fig. 8 was found to propagate at 730 m/sec, as compared with an estimated expansion speed for nitrogen of 1770 m/sec. The electrical discharge initiates at a region of high gas density in the arc chamber. The neutral gas total pressure decreases rapidly downstream of the chamber, to the extent that it is approximately at vacuum conditions at 30 cm from the anode, the data gathering region.

Typical Total Pressure Traces

Figure 9 shows typical 5-trace overlays of the total pressure signals for two different peak arc current cases, 7.4 kA and 13.4 kA. For both cases, low frequency pressure probe signals all show one common feature, the total pressure appears as a

single pulse, 18 to 20 μ sec wide, with at least an order of magnitude lower pressure thereafter for 100 to 200 μ sec. This later low pressure is not measurable with the present probe. The probe is somewhat acceleration sensitive and this alters the later part of the waveshape in a manner that is predictable but complicated. Consequently, only a qualitative interpretation will be given. In all the data to follow, only the peak pressure signal values will be discussed. The low frequency pressure probe has a relatively large sensing area. A check of the effect of probe area was made by examining the exhaust with the high frequency pressure probe (one-quarter the area of the low frequency probe). No differences in pressure amplitude or waveshape were noted.

The five-trace overlays of pressure serve to illustrate the amount of shot-to-shot data scatter. The 7.4 kA case shown in Fig. 9(a) shows severe scatter, even though the mass per shot is held to within 10 percent variation. At higher arc current (Fig. 9(b)) the scatter is not as serious. This is generally the case. The data of the remaining figures are 5-shot averaged to smooth this scatter.

The other set of simultaneous traces in Fig. 9 show Rogovsky loop signals at the same Z location. These signals provide an indication of the gross current in the plume that extends out from the thruster. The point to be noted here is the fact that the plume current occurs over 20 μ sec later than the pressure pulse. This point will be discussed later.

The pressure probe was also oriented so as to sense transient static pressure. It was found that this pressure was approximately an order of magnitude less than the corresponding total pressure for a particular station and thruster condition.

Phenomenology

The dominant pressure phenomenon in the exhaust for the first 100 to 200 microseconds is the narrow transient total pressure pulse. The second most important observation relates to the sequence of events occurring in the exhaust at a particular station. Rogovsky loops, Faraday cup probes, pressure probes, and results described in an earlier paper on laser scattering diagnosis of the exhaust were used jointly to determine this sequence of events. The sequence will be described at a particular station.

Exhaust light. - Exhaust light is the earliest signal to be observed at a specific station in the duct. In Fig. 10, the sequence of events is demonstrated with simultaneous records of static pressure and exhaust light at Z = 20 cm. Figure 10(a) is for a 7.4 kA peak arc current and 2.0 T magnetic field, and Fig. 10(b) is for 13.4 kA and 1.0 T. The waveshape in Fig. 10(b) is an early spike, a pedestal (lasting about the 40 μ sec) and a decaying section. This sequence was discussed earlier in Ref. 4.

Pressure pulse. - Following the light front is a narrow pulse of static pressure, from a few to ten microseconds later depending on thruster parameters (Fig. 10). A gas-kinetic (total) pressure pulse occurs near the time of the static pressure pulse. This pulse is shown in Fig. 11 for the

same conditions as in Fig. 10, but at Z = 30 cm.

Ion arrival. - Faraday cup signals (also shown in Fig. 11) indicate ion arrival at times later than the pressure pulse. Table 1 lists the time difference between initial occurrence of total pressure pulse and initial occurrence of Faraday cup signal (ion arrival) as the auxiliary magnetic field parameter is varied.

TABLE 1 TIME DIFFERENCE BETWEEN TOTAL PRESSURE AND ION ARRIVAL

Auxiliary magnetic field, T	Peak arc current, kA	Arrival time, μ sec		ΔT , μ sec
		Pressure signal	Faraday signal	
0	7.4	79	95	16
0	13.4	59	65	6
1.0	7.4	72	145	73
1.0	13.4	64	120	56
2.0	7.4	65	110	45
2.0	13.4	56	85	29

It lists the data for two peak arc current cases. An independent check of this behavior was made earlier and briefly described in Ref. 4. In that reference laser scattering diagnosis showed no significant electron number density until the Faraday cup signal arrival time. Thus Faraday signal arrival time (or electron number density initial occurrence) heralds the arrival of plasma at that station, much later than exhaust light and the total pressure pulse.

Plume currents. - The Rogovsky loop signals indicate current conduction in the exhaust. Significant current arrives much later than the pressure pulse. This is dramatically evident in Fig. 9 for Z = 25 cm. The result is much the same at 30 cm. Within the accuracy of these tests, the intense plume current onset is coincident with initial Faraday cup signals for a particular station.

Within the limitations of the several instruments used in gathering the data, the sequence of events at a particular station can be summarized as:

- (a) Exhaust light arrival,
- (b) Narrow total (and static) pressure pulse, arriving, a few microseconds later,
- (c) Ion arrival, or plasma arrival, tens of microseconds later,
- (d) Plume currents initiating at about the same time as (c), and
- (e) Decaying plasma conditions after (c).

This sequence is much like that which occurs in a transient plasma gun. However such guns have higher velocity current sheets (or plumes) and better structural plume definition. The current plume appears to act as a plow pushing neutral gas ahead of it. This large amplitude neutral gas pulse then dominates as the important component of impulse for at least 100 microseconds. That is, the thrust during this period is mostly due to a transient impulse rather than the steady "blowing" provided by steady-state thrusters. The pressure measurements show that the time integral pressure is dominated by a transient pulse for at least the period of 100 microseconds or so. This occurs even though

non-changing, or slowly-changing, terminal characteristics, light signals, or probe signals might have suggested the experiment was in a partly steady or quasi-steady realm. Thus, is a megawatt pulsed level MPD-ARC thruster is to simulate a steady MPD-ARC thruster, then it will have to be operated for longer pulse durations.

The time constant associated with attaining an impulse per shot that is dominated by steady "blowing," rather than transient pulse is clearly longer than the experiment times of this report.

Total Pressure Profiles

In this section the amplitude of the total pressure pulse is described for various auxiliary magnetic field cases and at various axial and radial stations. Only 5-shot averaged peak values of the pulse are described. The peak total pressure variation with applied magnetic field is considered prior to profile effects. This variation is shown in Fig. 12 for the case where the pressure probe is located at $r = 0$, $Z = 25$ cm, and the 5-shot averaged data is for one peak arc-current condition of 13.4 kA. The peak pressure ranged from 12,500 N/m^2 for no auxiliary magnetic field to 25,000 N/m^2 at 2.0 T. The mean deviation of the 5-shot average is shown (as an error bar) for each data point. There is some evidence that the peak pressure pulse amplitude saturates for magnetic field greater than 1.0 T. Similar mean deviations were evident in all the data of later figures but will not be shown to simplify the graphs.

Peak total pressure profiles are presented in Fig. 13. These are shown for three different axial positions down the duct, $Z = 25$ cm, 30 cm, and 35 cm, and for two different peak arc current cases, 7.4 kA and 13.4 kA. Magnetic field is the parameter.

For the no-field case, at $Z = 25$ cm, there is some evidence of a profile maximum at $r = 2$ cm. This profile flattens and decays farther downstream at $Z = 30$ cm and $Z = 35$ cm.

At 1.0 T magnetic field, the profile for the 7.4 kA condition still shows a maximum at $r = 2$ for $Z = 30$ cm and $Z = 35$ cm but has much larger values of peak pressure. For the 13.4 kA condition at $Z = 25$ cm, the peak total pressure at $r = 0$ is 21,000 N/m^2 . At this current condition, the profile shape inverts such that at the $r = 4$ cm position the pressure is higher valued than at $r = 0$ cm for $Z = 30$ cm, and $Z = 35$ cm.

At 2.0 T magnetic field, the peak total pressure for a corresponding case is only slightly higher showing the "saturation" effect with field more markedly than for the data of Fig. 12.

The inversion of the profile shape with increasing field noted above appears related to the effect of the magnetic field forcing ions (and ahead of the ions, neutrals swept up through collisions) to follow the expanding field lines rather than focusing them on centerline. This effect is more pronounced as the magnetic field is increased from 1.0 to 2.0 T at the 13.4 kA condition.

The pressure profile maxima at $r = 2$ cm for the self-field case and the 7.4 kA condition with

1.0 T field is not unexpected, since this is about the mid annulus position of the arc. This effect is seen to change at higher arc current, higher field cases, the influence of the auxiliary magnetic field altering the effect. Earlier work, involving laser scattering diagnosis of the plasma density that arrives later at that station⁽⁴⁾ evidences a much different profile effect. The self-field cases for plasma number density are somewhat the same profile as for pressure, but the field cases for plasma number density show a reduced density on axis, and a lower peak value of number density as magnetic field increases. The plasma arriving significantly later than the transient neutral pressure pulse thus exhibits different profile and trends as a function of magnetic field. Such behavior serves to emphasize the seriousness of accurately determining the time period of each measurement and identifying dominant effects.

The decay of total pressure profile with distance down the duct is expected to be influenced by the 15 cm diameter exhaust duct. At large axial distances the effect of magnetic nozzling appears difficult to examine in such a small diameter duct.

Pulse Velocity

The transit time for the total pressure pulse to pass by stations at $Z = 25$ and $Z = 35$ cm is used to calculate the pulse velocity. The resulting calculated velocity profiles are shown in Fig. 14. The 7.4 kA condition indicates velocities in the range from 5000 to 10,000 m/sec. Increasing the magnetic field again inverts the profiles with velocities at $r = 4$ cm larger for 1.0 T and even larger for 2.0 T. The higher current condition, 13.4 kA, evidences generally higher velocities. The profiles, except for the self-field case (which peaks at $r = 2$ cm) show inverted shapes for 1.0 and 2.0 T with the highest velocities at $r = 4$ cm.

Calculated Heavy Particle Number Density

Calculation of the heavy particle number density was carried out assuming Newtonian flow for the $z = 30$ cm position using the peak total pressure and the mean pulse velocity evaluated above. Since no ionized species are present in the region of maximum pressure, the density then can be attributed to neutral particles. Assuming then that total pressure is the simple product of density and the square of velocity, profiles of number density similar to those for velocity were derived. However, clearly definable trends are not evident, and so those results will not be presented here. Rather, when an average number density across the radial profiles is evaluated ($R = 0 - 4$ cm), an interesting variation with applied magnetic field can be observed (fig. 15). For the 7.4 kA condition the average number density in the front region can be seen to increase markedly, while in the 13.4 kA condition the swept density in the central core region is seen to decrease with applied field. Such conflicting trends provide strong evidence that the arc starting transient is quite sensitive to the magnetic field configuration.

The neutral number densities shown in Fig. 15 are about an order of magnitude larger than the plasma number densities⁽⁴⁾ measured in the sub-

sequent plasma portion of the flow.

Swept Mass in the Pressure Pulse

If the pulsed MPD-ARC is considered as a form of plasma gun for its initial transient period, an interesting question is the extent to which the current sheet "sweeps up" and accelerates the propellant. An efficient "sweep-up" for the transient pulse would make the thruster operate "gas-starved" for a time period while it rebuilds a stable mass flow again. A brief "gas-starved" condition could result in electrode erosion, and electrode material would be in the exhaust.

To examine the question of propellant sweeping, in the present experiment, an estimate was made of the amount of mass in the pressure pulse for one particular case, 13.4 kA peak arc current, and 1.0 T magnetic field. The pressure pulse amplitude and width for the radial profile measured at $Z = 25$ cm was approximately integrated to determine the mass in the pressure pulse. It was found to be about 10 percent of the mass of the propellant having left the thruster by that time. That is to say, the effect of the arc current sheet "sweep-up" is poor and should not cause a "starved" condition; the little electrode and insulator erosion noted supports such a conclusion in the present case. However, such a result does not preclude the possibility of more efficient sweeping in other cases.

Conclusions

Measurements of transient pressure and velocity were made for a megawatt, pulsed MPD-ARC thruster, operating single shot. These measurements and some earlier work using laser scattering diagnosis on the exhaust have aided in drawing the following general conclusions;

1. In the initial exhaust, there is a narrow (tens of microseconds wide) transient total pressure pulse which dominates the time integral pressure for over 100 microseconds. Thus, the impulse provided by the thruster for this initial period is dominated by this pulse.

2. If the transient pressure component of the exhaust impulse dominates over the steady "blowing" component, the total impulse cannot be considered a steady or quasi-steady thrust condition. This is the case for the megawatt-level pulses studied in this paper. Much longer powering times will have to be used to insure steady thrusting is the dominant condition.

3. The sequence of events at a given station in the exhaust for a single shot megawatt-level MPD-ARC thruster is:

- a. Exhaust light arrives
- b. After a few microseconds, a narrow (20 microseconds wide) total pressure pulse of neutral gas passes
- c. Arc current sheet (plume) arrives tens of microseconds later, and at the same time that plasma is first detected.
- d. A flowing plasma is noted.

4. Auxiliary magnetic field increases the initial peak transient total pressure pulse up to 2.0 T where some degree of "saturation" is noted.

At 2.0 T, the pressure profiles suggest that the magnetic field directs some of the ions (and thus some neutrals by collisions) outward toward the duct wall.

Acknowledgement

The assistance of Mr. Ronald R. Robson in providing instrumentation and operations engineering support is greatly appreciated.

References

1. Clark, K. E., "Quasi-Steady Plasma Acceleration," Aerospace and Mechanical Sciences Report No. 859, May 1969, Princeton University, Princeton, N.J.
2. Lovberg, R., "Physical Processes in the Magneto-Plasmadynamic Arc," Second Semiannual Report, NASA CR-83891, Mar. 1967, University of California, San Diego, La Jolla, Calif.
3. Ashby, D. E. T. F., Liebing, L., and Larson, A. V. and Gooding, T. J., "Quasi-Steady State Pulsed Plasma Thrusters," AIAA Journal, Vol. 4, No. 5, May 1966, pp. 831-835.
4. Michels, C. J. and Sigman, D. R., "Exhaust Characteristics of a Megawatt Nitrogen MPD-ARC Thruster," Paper 70-1081, Aug. 1970, AIAA, New York, N.Y.
5. Clark, K. E. and Jahn, R. G., "Quasi-Steady Plasma Acceleration," AIAA Journal, Vol. 8, No. 2, Feb. 1970, pp. 216-220.
6. Jahn, R. G., Clark, K. E., Oberth, R. C., and Turchi, P. J., "Acceleration Patterns in Quasi-Steady MPD ARCS," Paper 70-165, Jan. 1970, AIAA, New York, N.Y.
7. Turchi, P. J. and Jahn, R. G., "The Cathode Region of a Quasi-Steady MPD ARC Jet," Paper No. 70-1094, AIAA, Aug. 1970, New York, N.Y.
8. Clark, K. E., DiCapua, M. S., Jahn, R. G., and Von Jaskowsky, W. F., "Quasi-Steady Magneto-plasmadynamic Arc Characteristics," Paper No. 70-1095, AIAA, Aug. 1970, New York, N.Y.
9. Jahn, R. G., Von Jaskowsky, W. F., and Clark, K. E., "Pulsed Electromagnetic Gas Acceleration," 15th Semiannual Progress Report, NASA Grant No. NGL 31-001-005, Supplement 7, Jan. 1, 1970, Princeton University, Princeton, N.J.
10. Hoell, J. M., Burlock, J., and Jarrett, O., Jr., "Velocity and Thrust Measurements in a Quasi-Steady Magnetoplasmadynamic Thruster," Paper No. 70-1080, AIAA, Aug. 1970, New York, N.Y.
11. Michels, C. J., "Dynamic Current-Voltage Characteristics of a Megawatt MPD-ARC Thruster," Paper No. 70-164, AIAA, Jan. 1970, New York, N.Y.

12. Kribel, R. E., "Plasma Transport in a Magnetoplasma-dynamic Arc," Ph.D. Dissertation, 1968, University of California, San Diego, Calif.
13. Malliaris, A. C. and John, R. R., "Outstanding Problems Regarding the Feasibility of a Repetitively Pulsed MPD Propulsion System," Paper No. 70-1093, AIAA, Aug. 1970, New York, N.Y.
14. York, T. M., "Pressure Distribution in the Structure of a Propagating Current Sheet," Department of Aerospace and Mechanical Sciences Report No. 853, Dec. 1968, Princeton University, Princeton, N.J.
15. York, T. M., "Stress Dynamics in High Speed Piezoelectric Pressure Probes," Review of Scientific Instruments, Vol. 41, No. 4, Apr. 1970, pp. 519-521.

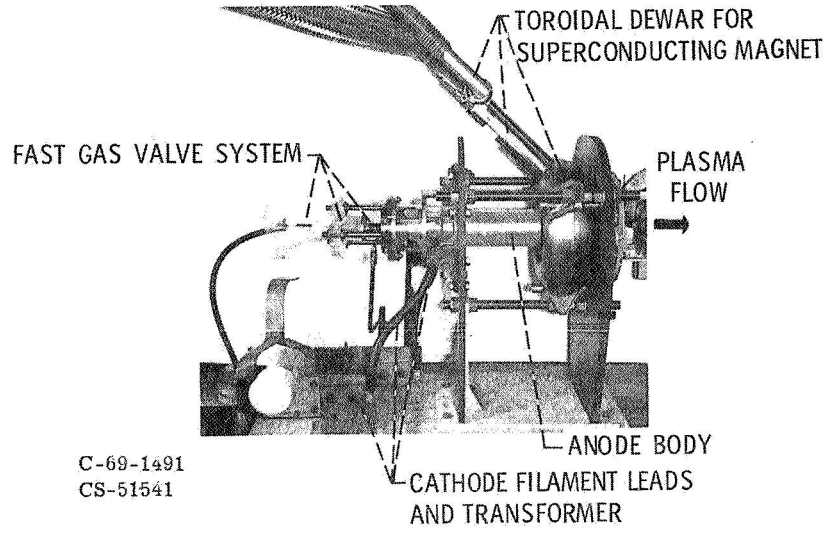


Figure 1. - Megawatt MPD-arc plasma source.

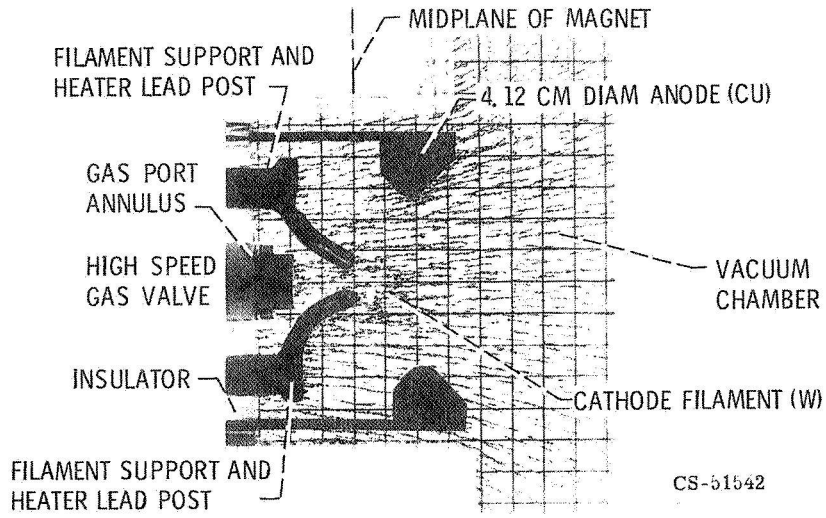


Figure 2. - Arc chamber.

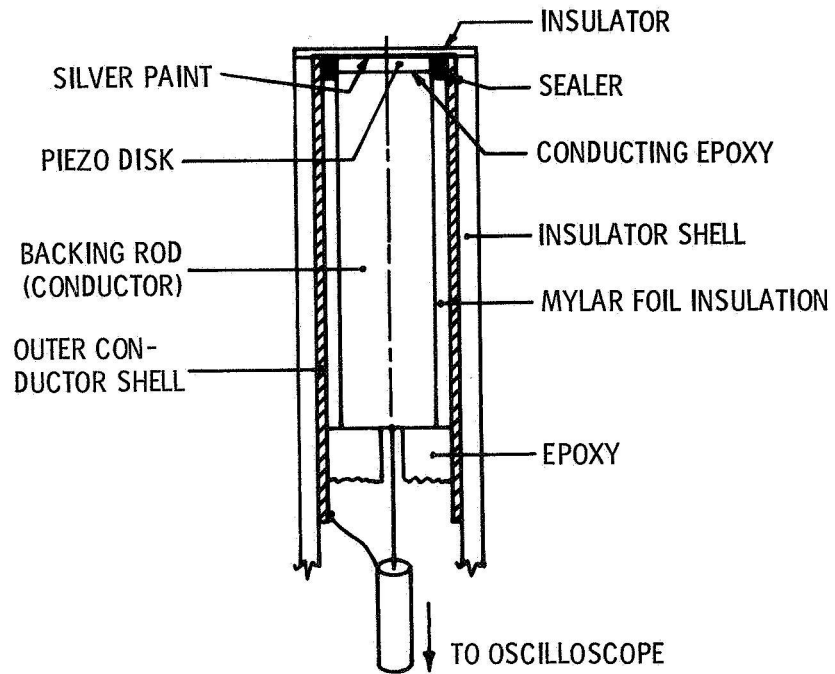


Figure 3. - Cross section sketch of piezoelectric pressure probe.

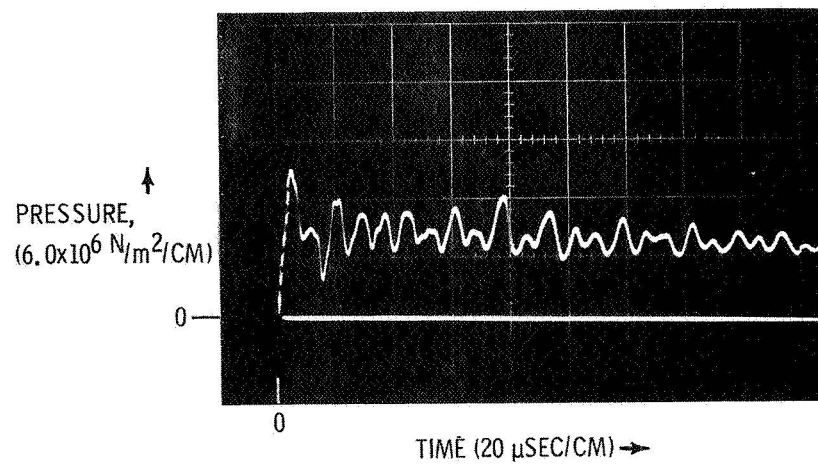


Figure 4. - Shock tube pressure signal.

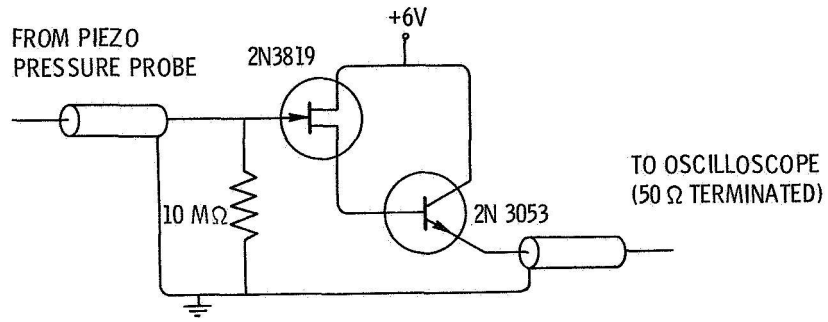


Figure 5. - Emitter follower circuit.

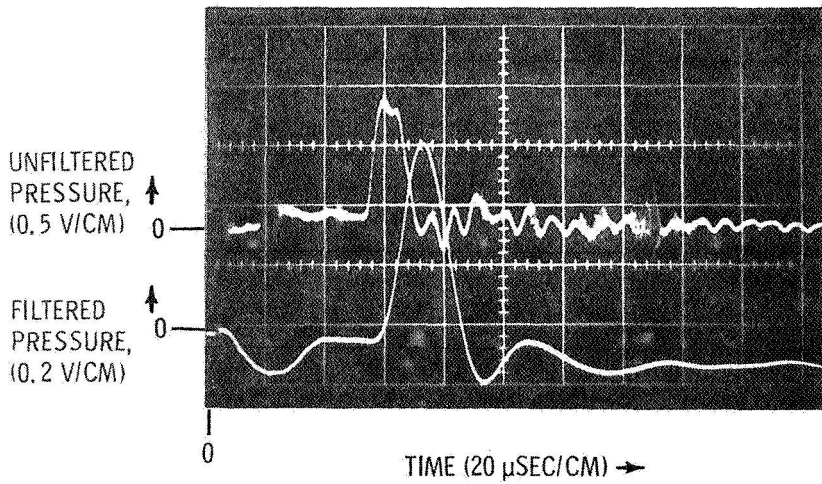


Figure 6. - Comparison of filtered and unfiltered pressure signals.

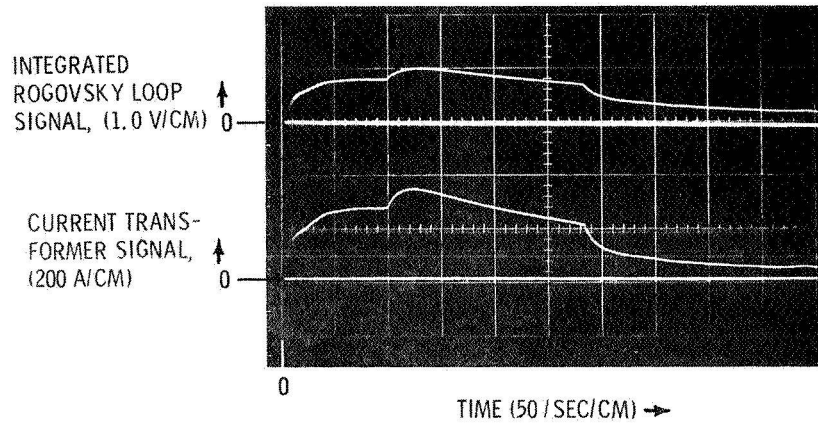


Figure 7. - Rogovsky loop calibration traces.

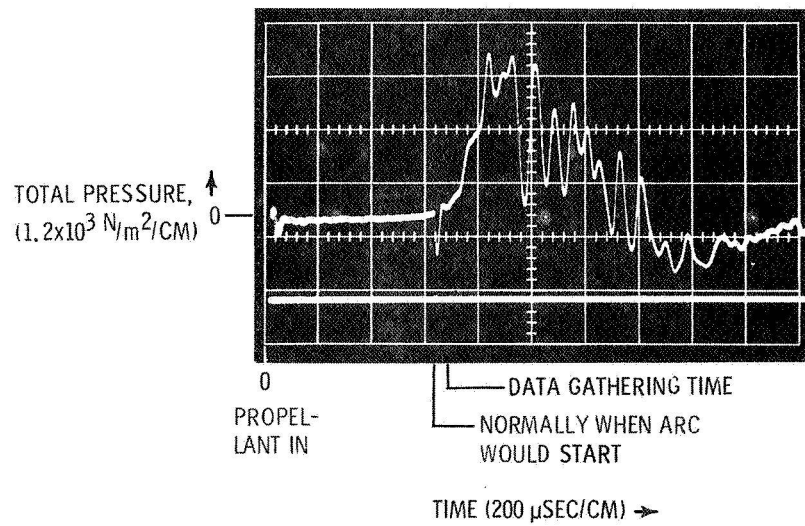
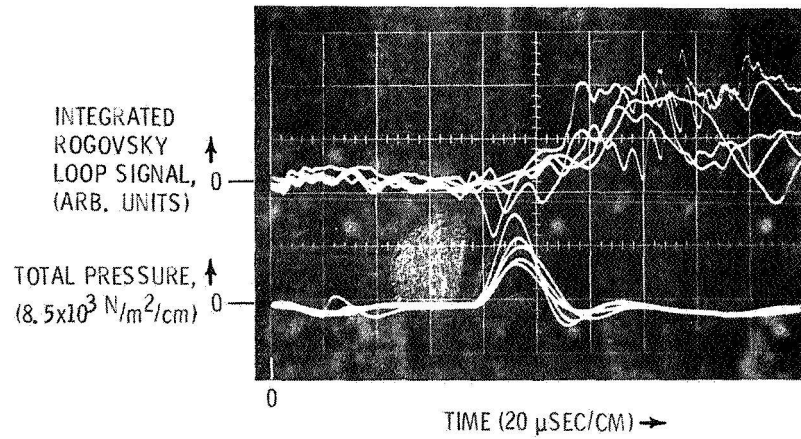
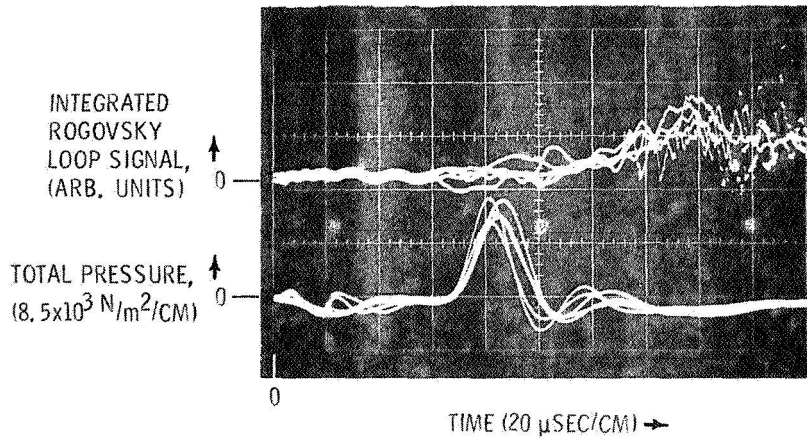


Figure 8. - Total pressure (unfiltered), cold gas flow at $z = 30 \text{ cm}$, $R = 0$.



(a) 5-Trace overlays for 7.4 kA, 1.0 T case (Rogovsky loop at $r = 4 \text{ cm}$, $z = 25 \text{ cm}$ and pressure probe at $r = 0$, $z = 25 \text{ cm}$).



(b) 5-Trace overlays for 13.4 kA, 1.0 T case (Rogovsky loop at $r = 4 \text{ cm}$, $z = 25 \text{ cm}$ and pressure probe at $r = 0$, $z = 25 \text{ cm}$).

Figure 9. - Typical total pressure and Rogovsky loop traces.

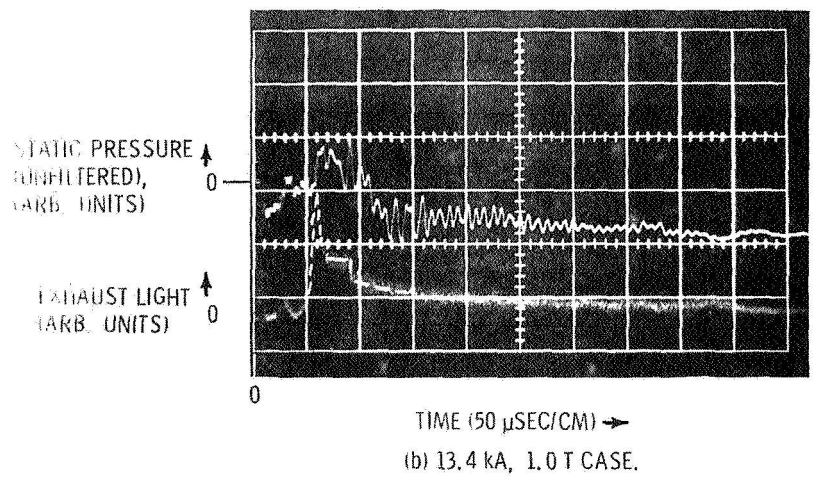
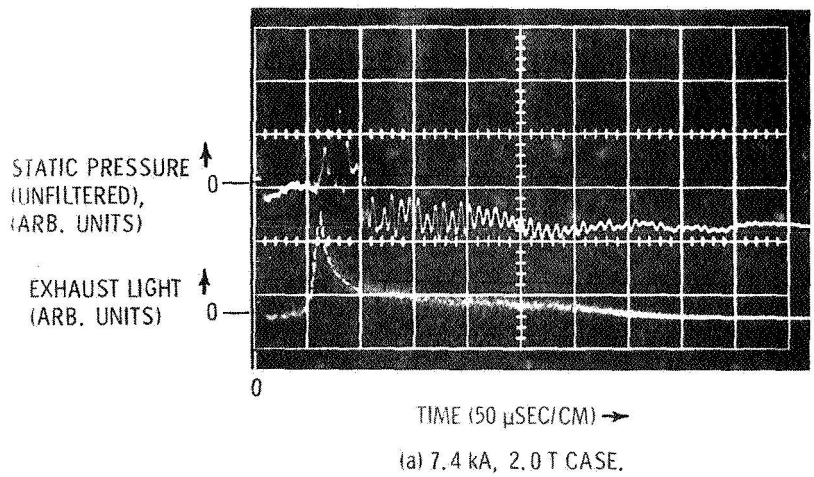


Figure 10. - Simultaneous exhaust light and static pressure signals at $z = 20$ cm.

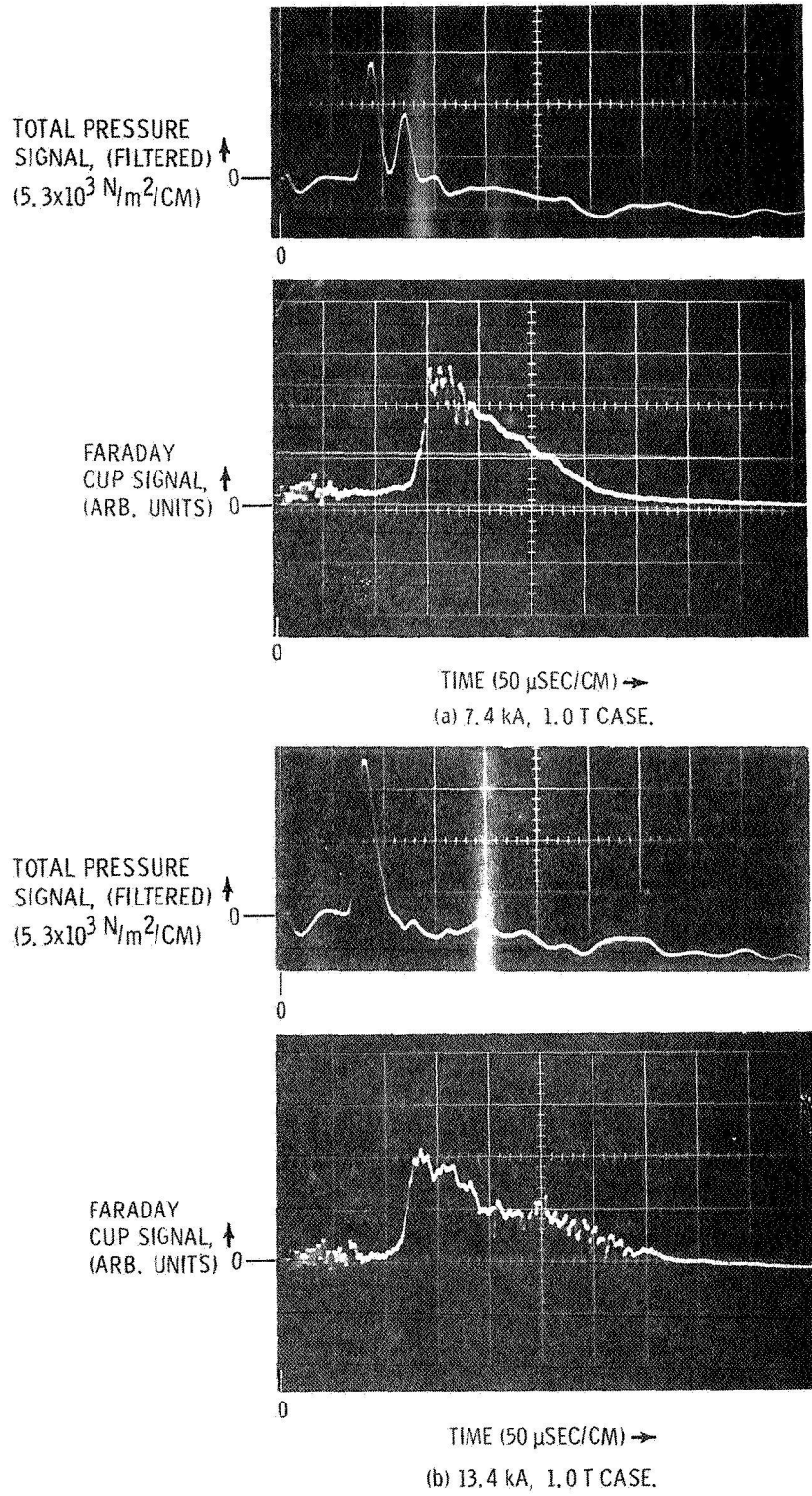


Figure 11. - Simultaneous total pressure and Faraday Cup signals at $z = 30 \text{ cm}$.

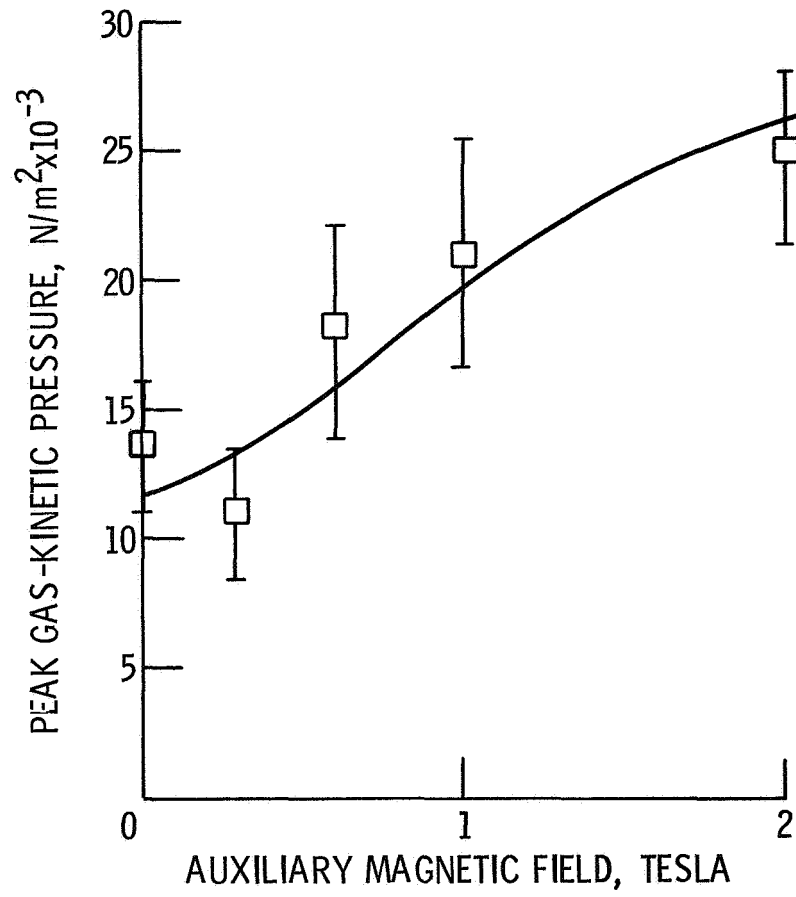


Figure 12. - Peak gas-kinetic pressure variation with applied magnetic field at $r = 0$, $z = 25$ cm, for 13.4 kA case.

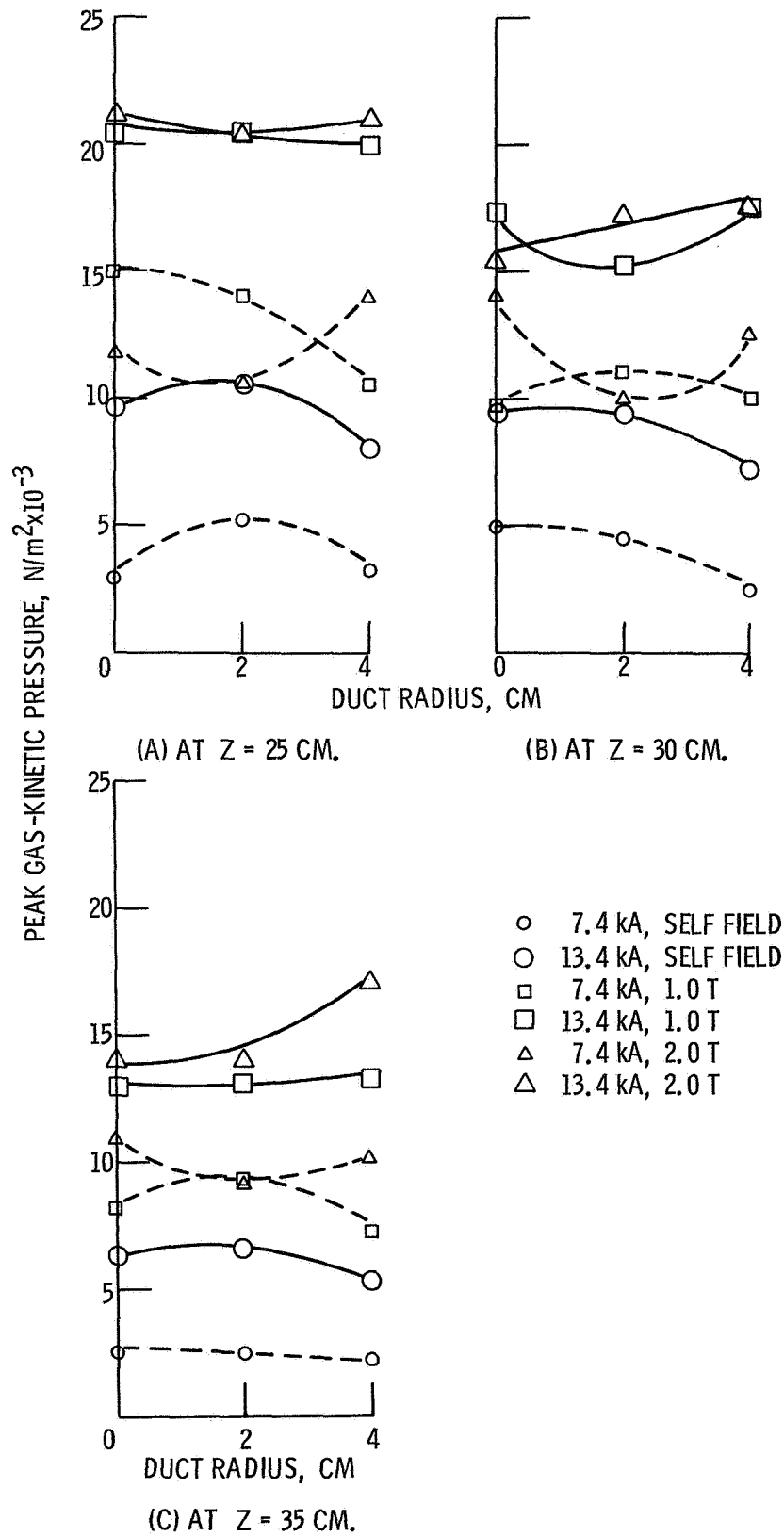


Figure 13. - Peak gas-kinetic pressure profiles.

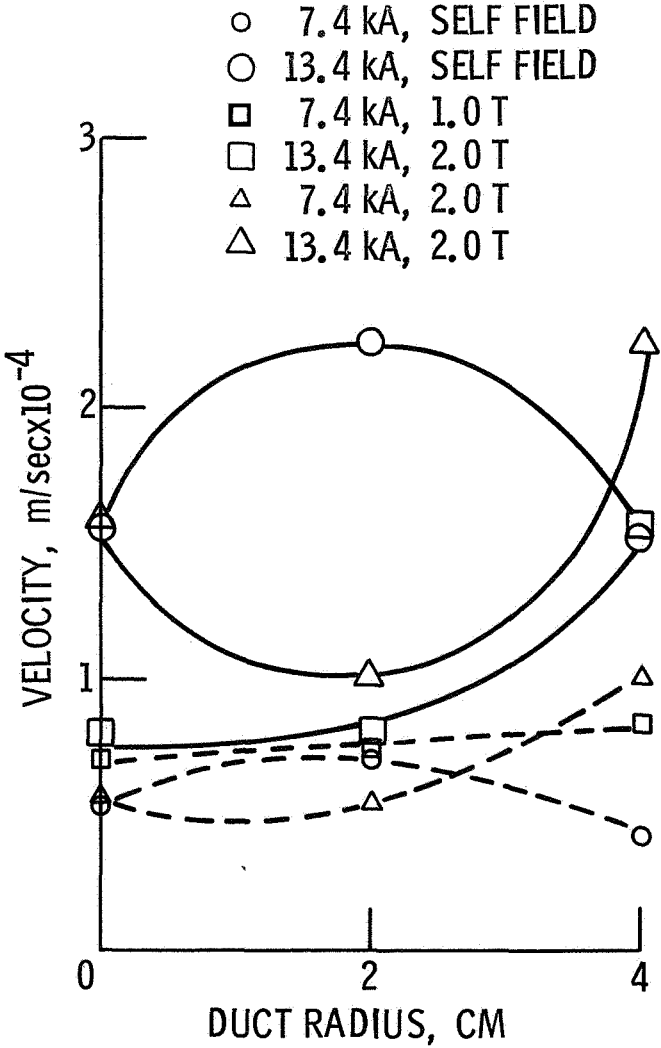


Figure 14. - Pulse velocity profiles at z = 30 cm.

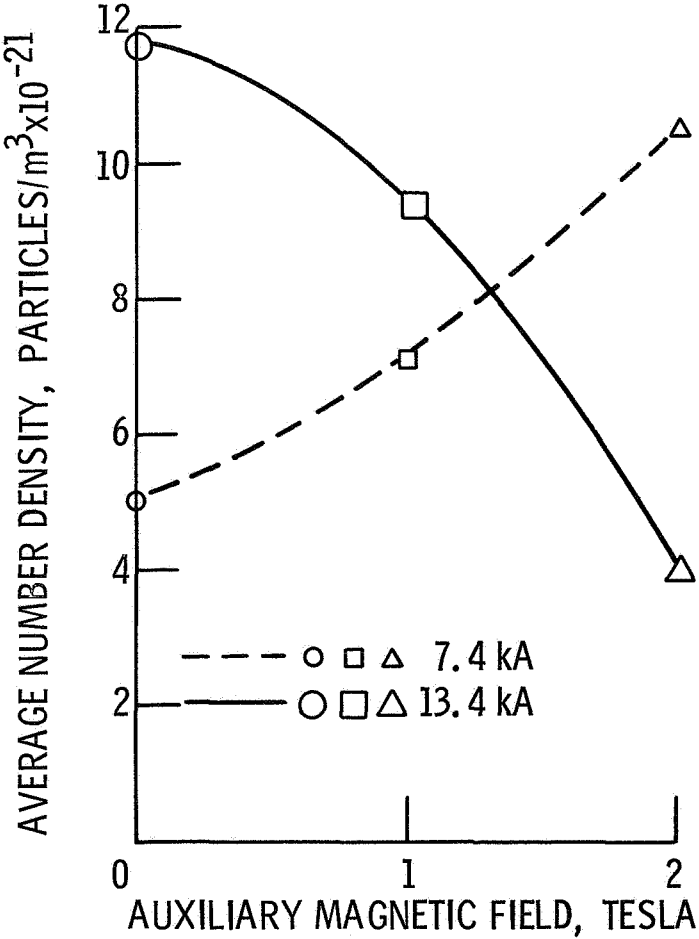


Figure 15. - Average number density variation with applied magnetic field.